High-pressure structural behaviour of silver(I) fluoride

1998 J. Phys.: Condens. Matter 10 7945

(http://iopscience.iop.org/0953-8984/10/36/005)

J. Phys.: Condens. Matter **10** (1998) 7945–7955. Printed in the UK PII: S0953-8984(98)94560-X

High-pressure structural behaviour of silver(I) fluoride

S Hull† and P Berastegui

The ISIS Facility, Rutherford Appleton Laboratory, Chilton, Didcot, Oxon OX11 0QX, UK

Received 26 May 1998, in final form 9 July 1998

Abstract. The high-pressure structural behaviour of AgF has been studied by the powder neutron diffraction technique. The material undergoes a pressure-induced transition at 2.70(2) GPa from the rocksalt structure to the CsCl-type arrangement with a volume change of ∼10%. On decreasing pressure, the reverse CsCl → rocksalt transition occurs via an intermediate phase possessing the hexagonal anti-NiAs structure. A plausible structural model to explain this observation is provided, together with a discussion of the relative stability of the (anti-) NiAs arrangement as a high-pressure polymorph in binary MX compounds.

1. Introduction

The seven binary monohalides formed by copper and silver can be considered as 'I–VII' compounds which are ionic counterparts to the group IV and III–V semiconductors. However, their bonding character is not purely ionic and the I–VII compounds span the boundary between predominantly covalent systems characterized by fourfold coordinated structures and ionic ones possessing sixfold coordinated arrangements. At ambient temperature and pressure CuCl, CuBr, CuI and AgI adopt the tetrahedrally coordinated cubic zincblende structure (although the latter can also exist indefinitely in the hexagonal equivalent wurtzite arrangement) whilst AgF, AgCl and AgBr adopt the octahedrally coordinated rocksalt structure [1]. The structural behaviour of these systems under compression has been extensively studied using both experimental and theoretical approaches (see [2–8] and references therein). Hydrostatic pressure favours transitions to more densely packed structures and the increasing coordination numbers is, therefore, associated with changes in the bonding character. The prediction of these effects has proved a popular challenge for testing models of the interionic potentials, although principal emphasis has been placed on the transition from fourfold to sixfold coordinated structures [7, 9–12]. In contrast, the high-pressure structural behaviour of I–VII compounds beyond the octahedrally coordinated arrangements has only recently been addressed for the first time [8].

In the extensive compressibility studies of 27 binary monohalides by Vaidya and Kennedy [13], AgF was remarked to be 'among the most puzzling substances investigated'. On increasing pressure, a single phase transition was observed at 2.75 GPa whilst two transitions occurred on decompression, at 2.48 GPa and 1.79 GPa. Subsequent x-ray diffraction studies by Halleck *et al* [14] indicated that, on increasing pressure, the structural transition is from the ambient temperature rocksalt structure (AgF-I) to the eightfold coordinated CsCl-type structure (AgF-II) with a lattice constant $a_0 = 2.945$ Å. However, no

† E-mail address: sh@isise.rl.ac.uk.

0953-8984/98/367945+11$19.50

information concerning the behaviour on decreasing pressure was reported until the work of Jamieson *et al* [15] who observed an intermediate phase (labelled AgF-III) stable between AgF-II and AgF-I which could not be nucleated on increasing pressure despite extensive attempts. 12 Bragg peaks were measured by x-ray diffraction and used to determine a hexagonal unit cell of dimensions $a = 3.246(2)$ Å and $c = 6.23(4)$ Å. Probable space groups $P6_3/mmc$ and $P6_3mc$ were proposed, leading to a possible structural assignment of an inverse NiAs arrangement.

This paper describes powder neutron diffraction studies of AgF to ∼6.5 GPa, which probe in detail its high-pressure structural behaviour. In comparison to x-rays, neutrons have the advantage of using a somewhat larger sample (ensuring a better polycrystalline average and lower sensitivity to non-hydrostatic stress conditions) and remove the possibility of radiation damage to the sample during the experiment (all Ag^+ halides are light sensitive). Conversely, neutrons are less able to differentiate between Ag and F nuclei, because their coherent scattering lengths are relatively similar ($b_{Ag} = 5.922$ fm, $b_F = 5.654$ fm [16]). Silver also has a significant absorption cross section for thermal neutrons ($\sigma_{abs,Ag} = 63.3 \times 10^{-24}$ cm^2), though this is relatively unimportant with the small sample size used in these experiments.

2. Experimental details

Commercially available AgF of stated purity 99.999% purity supplied by the Aldrich Chemical Co was used in these experiments. The sample was dried under vacuum for ∼6 h at 420 K and handled under subdued lighting in an argon atmosphere. AgF is known to react with moisture to form the oxide via the reaction $2AgF + 2H_2O \rightarrow 2AgOH + 2HF \rightarrow Ag_2O + H_2O + 2HF$. The high-pressure experiments were performed using an opposed anvil pressure cell with a sample volume of ∼100 mm^3 [17]. Solid pellets were formed by pressing the material to ∼0.1 GPa. Pressure calibration was determined using a mixed sample of AgF + NaCl (in the approximate ratio 1:1 by volume) and the equation of state of NaCl given by Decker [18]. Diffraction experiments were performed on the Polaris powder diffractometer at the ISIS spallation neutron source, UK [19]. Detector banks covering the scattering angles $84^\circ < \pm 2\theta < 96^\circ$ collect diffraction data by the time-of-flight technique over the d-spacing range 0.5 Å $< d <$ 4.2 Å with an essentially constant resolution of $\Delta d/d \sim 0.5\%$. Typical counting times were ∼1 h for pressure calibration purposes, but longer collection times (∼10 h) were used to collect diffraction data of sufficient statistical quality for full structural refinement. The diffraction data were corrected for the effects of beam attenuation by the cell components and within the sample itself. Rietveld refinements to determine the crystal structure used the computer program TF12LS and its multiphase derivative [20], which are based on the Cambridge Crystallographic Subroutine Library [21].

3. Results

On increasing pressure the rocksalt structured phase AgF-I was observed to transform at a pressure $p = 2.70(2)$ GPa to the CsCl arrangement characteristic of phase AgF-II. This is in accord with the previous study of Halleck *et al* [14], who observed the transition at ∼2.6 GPa. The change in the unit cell volume at the transition is found to be $\Delta V_{I \rightarrow II}/V_I = -10.2(3)\%$. On decreasing pressure the CsCl structured phase remains stable at pressures down to $p = 2.71(2)$ GPa, at which point additional peaks at d-spacing

values of $d \sim 2.56$ Å, 1.67 Å and 1.62 Å appear. On further reducing the pressure to 2.59(2) GPa, the remaining peaks associated with phase AgF-II disappear but no peaks characteristic of the rocksalt structured ambient pressure phase AgF-I are present. The Bragg peaks now observed from the new phase could be indexed on a preliminary hexagonal unit cell with $a = 3.244(2)$ Å and $c = 6.24(1)$ Å. These values are in good agreement with those measured by Jamieson *et al* [15] and we therefore conclude that the diffraction data correspond to the same phase (labelled AgF-III) observed in their work. On further decrease in pressure, AgF-III reverts to rocksalt structured AgF-I at a pressure $p = 0.9(1)$ GPa. The compressibility of the three solid phases of AgF, illustrated in figure 1, gives values of 61(2), 110(5) and 71(3) for the isothermal bulk moduli at zero pressure (B_0) of AgF-I, AgF-II and AgF-III, respectively.

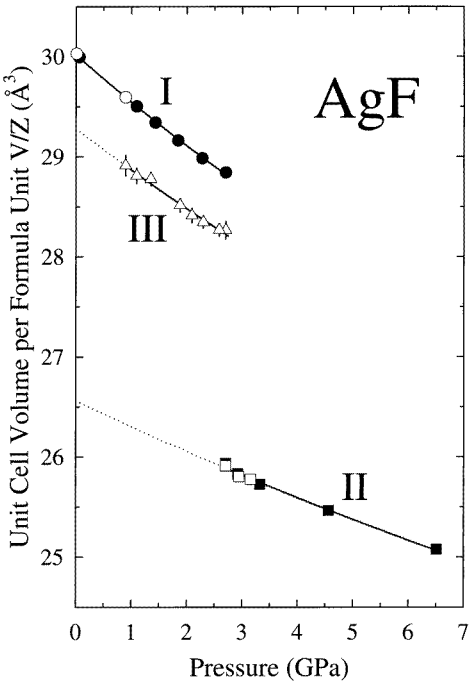

Figure 1. The compressibility of the three phases of AgF. The full and open symbols correspond to increasing and decreasing pressure measurements, respectively. The full curves represent a fit to the data using a first-order Birch equation [35] to determine the bulk moduli at zero pressure (B_0). The dotted lines are extrapolations of the curves to zero pressure.

Although the d-spacing range over which Bragg peaks can be isolated is slightly limited (by overlap of neighbouring peaks at $d < \sim 0.7$ Å and excessive absorption at $d > \sim 3.0$ Å), the apparent conditions for the presence of reflections are $l = 2n$ for both $00l$ and hhl sets. These conditions imply that the space group is either $P6_3/mmc$, $P\bar{6}2c$ or $P6_3mc$. The unit cell volume indicates that two formula units are located within the unit cell and, on these grounds, the most likely structural arrangements are wurtzite (both atoms in $2(b)$ positions of space group $P6_3mc$ at $(\frac{1}{3}, \frac{2}{3}, z)$ and $(\frac{2}{3}, \frac{1}{3}, z + \frac{1}{2})$ with $z = 0$ and $z \sim \frac{3}{8}$) or NiAs-type (space group $P6_3/mmc$ with one species in $2(a)$ sites at $(0, 0, 0)$ and $(0, 0, \frac{1}{2})$ and the other in $2(c)$ sites at $(\frac{1}{3}, \frac{2}{3}, \frac{1}{4})$ and $(\frac{2}{3}, \frac{1}{3}, \frac{3}{4})$). Given the similarity of the neutron

scattering lengths for Ag^+ and F^-, it is reasonable to establish the general positions of the ions by performing calculations with two identical 'ions' of average scattering length $b = (b_{Ag} + b_F)/2 = 5.788$ fm, returning to the question of the ordering of the two species over these positions shortly. Simulations of the diffraction patterns expected for wurtzite and NiAs-structured arrangements for AgF-III proved the latter to be the most promising candidate, the former severely overestimating the intensity of reflections such as 100 and 112 and underestimating ones such as 102.

Time-of-flight Rietveld refinements of the experimental data collected from pure AgF at $p = 2.10(2)$ GPa using the 'average' arrangement of Ag^+ and F^- provided an acceptable fit to the data, with a goodness-of-fit value $\chi^2 = 1.22$. The model corresponds to a disordered distribution of cations and anions over the available $2(a)$ and $2(c)$ sites. Subsequent refinements adopting ordered arrangements place the Ag^+ on $2(a)$ site and F^- on the $2(c)$ site (NiAs arrangement) and with the locations of the two species interchanged (anti-NiAs structure). The former gave a marginally poorer fit to the data ($\chi^2 = 1.26$) and the latter a slightly better one ($\chi^2 = 1.20$). In its most general case, the NiAs structure does not possess a mirror plane perpendicular to the c-axis and the true structure is described by space group $P6_3mc$. In the anti-NiAs case, the anions are in $2(a)$ sites at $(0, 0, z_F)$ with $z_F = 0$ to fix the origin and the cations in $2(b)$ sites at $(\frac{1}{3}, \frac{2}{3}, z_{Ag})$ with z_{Ag} close to (but not necessarily equal to) the value $\frac{1}{4}$. Attempts to refine the diffraction data in this lower symmetry case failed to give a significant improvement to the quality of the fit or to vary the value of z_{Ag} significantly away from the value $\frac{1}{4}$. On the basis of the neutron diffraction data, we therefore conclude that the best description of the structure of phase AgF-III is an anti-NiAs arrangement in space group $P6_3/mmc$. The fit to the data is illustrated in figure 2 and the results of the least-squares refinement are summarized in table 1.

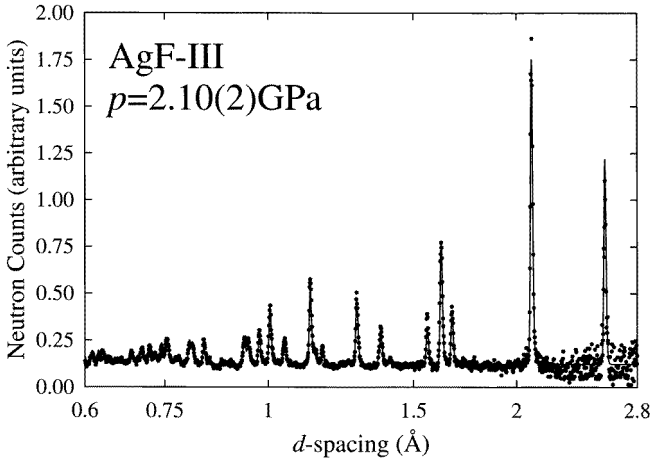

Figure 2. A least-squares fit to the diffraction data for the anti-NiAs-structured phase AgF-III collected at $p = 2.10(2)$ GPa. The dots are the experimental data points and the full curve line is the calculated profile using the fitted parameters listed in table 1.

However, it is important to note that the difference in the quality of fit to the neutron data using the ordered and disordered arrangements of Ag^+ and F^- is relatively small. To confirm the assignment of the anti-NiAs configuration we can use the greater sensitivity of the x-ray diffraction technique to differentiate between the two species. Table 2 shows the calculated x-ray intensities of the diffraction lines using the structural parameters determined

Table 1. Summary of the results obtained by least-squares refinement of the diffraction data collected for the anti-NiAs structured AgF-III at $p = 2.10(2)$ GPa.

Phase	AgF-III
Pressure	$p = 2.10(2)$ GPa
Temperature	$T = 295(2)$ K
Structure	anti-NiAs
Space group	$P6_3/mmc$
Unit cell constants	$a = 3.2434(1)$ Å
	$c = 6.2386(2)$ Å
	$c/a = 1.9235(1)$
Formula units per unit cell	$Z = 2$
Unit cell volume	$V/Z = 28.412(2)$ Å^3
Anions	F^- in $2(a)$ sites at $0, 0, 0$ and $0, 0, \frac{1}{2}$
	$B_F = 0.23(12)$ Å^2
Cations	Ag^+ in $2(c)$ sites at $\frac{1}{3}, \frac{2}{3}, \frac{1}{4}$ and $\frac{2}{3}, \frac{1}{3}, \frac{3}{4}$
	$B_{Ag} = 0.33(14)$ Å^2
Weighted profile R-factor	$R_{wp} = 2.42\%$
Expected R-factor	$R_{exp} = 2.21\%$
Goodness-of-fit	$\chi^2 = 1.20$
Number of data points	$N_d = 1934$
Number of Bragg peaks	$N_B = 140$
Number of fitted parameters	$N_p = 11$

Table 2. Comparison of the observed intensities of the diffraction peaks measured by x-ray diffraction reported by Jamieson *et al* (I_{obs}) [15] with those calculated using anti-NiAs, NiAs and disordered structural models. The latter considers the Ag^+ and F^- to be randomly distributed over the $2(a)$ and $2(c)$ sites of the NiAs structure.

			$100 \times I_{calc}/I_{max}$		
hkl	d_{calc} (Å)	I_{obs} [15]	Anti-NiAs	NiAs	Disordered
002	3.119	S	28.8	37.7	0.0
100	2.809	—	9.7	100.0	17.7
101	2.561	VVS	100.0	4.2	75.8
102	2.087	S	26.1	89.6	100.0
103	1.671	S	15.3	0.5	11.7
110	1.622	S	11.7	15.2	26.7
004	1.560	—	3.1	4.1	7.1
112	1.439	M	6.6	8.6	0.0
200	1.409	—	0.5	4.4	0.8
201	1.370	M	5.0	0.2	3.9
104	1.364	—	0.9	7.3	1.3
202	1.281	W	1.8	6.5	7.5
203	1.164	W	1.8	0.1	1.3
105	1.140	W	1.5	0.0	1.2
114	1.124	W+	2.4	3.1	5.7
120	1.062	—	0.2	1.5	0.3
121	1.047	W^+	1.8	0.1	1.3
204	1.044	—	0.2	1.3	0.2

by the neutron diffraction study (table 1). The calculated values for the two ordered and one (fully) disordered models are compared with the measured intensities quoted by Jamieson *et al* [15], taking the strongest measured line (101) as an intensity of 100.0. Only the

ordered anti-NiAs arrangement successfully accounts for the distribution of intensities and we conclude that this is the correct structural description for AgF-III.

4. Discussion

The anti-NiAs arrangement of AgF-III comprises of two interpenetrating sublattices, an almost ideal hexagonal-close-packed Ag^+ array and a simple hexagonal F^- one. Whilst both ionic species are six coordinated to unlike neighbours, the anion and cation environments are different in the anti-NiAs structure, unlike the case in the rocksalt and CsCl structures. The Ag^+ lie at the centre of a trigonal prism formed by $6 \times F^-$ and the F^- are surrounded by an octahedron of $6 \times Ag^+$, although there are an additional $2 \times F^-$ at a distance $c/2$ along the [001] direction. The Ag^+–F^- distance of ∼2.44 Å is intermediate between the values of ∼2.42 Å and ∼2.55 Å observed in the neighbouring rocksalt and CsCl-structured phases, respectively, suggesting that the bonding remains predominantly ionic in AgF-III. The value of the single positional parameter z_{Ag} displaces the cation sublattice relative to the anion one parallel to the z-axis. The refined value of $z_{Ag} = \frac{1}{4}$ places the Ag^+ and F^- at the centres of their respective trigonal prisms and octahedra, as might then be expected for essentially spherical ions.

The variability of the values of the unit cell axis ratio c/a and the positional parameter z make the (anti-) NiAs structure highly versatile, especially in those cases where the bonding character is intermediate between metallic and ionic or between metallic and covalent [1, 22]. However, whilst many chalcogenides, phosphides and arsenides compounds adopt the NiAs arrangement, the reasons for its adoption in preference to other binary MX structures are not well understood [22]. Indeed, in many cases, the ideal NiAs structure has been shown to be a simplification of the true crystal structure, being prone to non-stoichiometry and the formation of complex superlattices and subtle distortions (as in the case of NiAs itself [23]). However, in the case of AgF-III presented in this work, we find no evidence of distortions from hexagonal symmetry and the anti-NiAs description appears to be wholly appropriate. Similarly, we observe no splitting of the diffraction lines into two sets as reported by Jamieson *et al* [15] after the application of pressure and interpreted as the formation of two non-stoichiometric phases, one Ag^+ rich and the other F^- rich.

The relationship between the (anti-) NiAs and rocksalt structures has been discussed previously [24]. In a monatomic solid, it is well known that simple hexagonal layers of atoms can be stacked to form three-dimensional close-packed structures with a layer sequence ABABAB... and ABCABCABC... [1]. The former is hexagonal close packed (hcp) and the latter cubic close packed (ccp). Similarly, in a binary solid (using upper case characters to denote the anions and lower case ones the cations) the tetrahedrally coordinated wurtzite and zincblende structures can be described as hexagonal and cubic counterparts, i.e.

zincblende AaBbCcAaBbCcAaBbCc...

wurtzite AaBbAaBbAaBbAaBbAa....

If the same cubic → hexagonal transformation is applied to the octahedrally coordinated rocksalt structure

rocksalt AbCaBcAbCaBcAbCaBc...

we obtain the NiAs arrangement

NiAs AbCbAbCbAbCbAbCbAb...

with hcp anions (ACACAC...) and simple hexagonal cations (bbbbbb...). In the ideal case, the NiAs structure has $c/a = \sqrt{8/3} = 1.633$ and the positional parameter $z = \frac{1}{4}$. The relationship between the cubic unit cell parameter of the rocksalt structure, a_{RS} and the hexagonal unit cell constants of the NiAs structure, a_{NiAs} and c_{NiAs}, are $a_{NiAs} = a_{RS}/\sqrt{2}$ and $c_{NiAs} = 2a_{RS}/\sqrt{3}$. In practice, many NiAs-structured compounds have $c/a < \sqrt{8/3}$, due to the attraction between the metal atoms situated in neighbouring simple hexagonal layers at a distance $c/2$ along the z-axis. This is associated with a tendency to form a metallic bond [22]. In the case of the anti-NiAs-structured phase AgF-III, the value $c/a \sim 1.92$ is significantly larger than the ideal, presumably due to electrostatic repulsion between the like-charged F^- at a distance $c/2$. As discussed later in this section, this distinction has important consequences in explaining the different behaviour of AgF compared to 'normal' NiAs-structured compounds.

It is well known that the rocksalt $\rightarrow$ CsCl transition can, in principle, be continuous [25–27]. The most straightforward mechanism involves only a $\langle 111 \rangle$ distortion of the primitive rhombohedral unit cell (see figure 3). Indeed, such a route has been proposed to occur in AgCl and AgBr under hydrostatic pressure on the basis of recent total energy calculations using the local density approximation [8]. However, the rocksalt $\rightarrow$ CsCl transition observed at $p = 2.70(2)$ GPa in AgF appears to be first order, with a volume ratio at the transition of $V_{CsCl}/V_{RS} = 0.898(2)$. Since the compound is predominantly ionic in character, it is reasonable to treat the ions as 'hard spheres' of the ionic radii, where $r_{Ag^+} = 1.15$ Å and $r_{F^-} = 1.33$ Å for sixfold coordination [28]. For a binary MX compound, the fraction V_{CsCl}/V_{RS} is dependant on the ratio of the radii of the two species r_M/r_X in the manner described in table 3. The CsCl structure is more densely packed than the rocksalt one only if $r_M/r_X > 0.587$, but reaches a limiting value $V_{CsCl}/V_{RS} = 0.770$ when $r_M/r_X \geqslant 0.732$. In these circumstances, the two structures are characterized by contacts

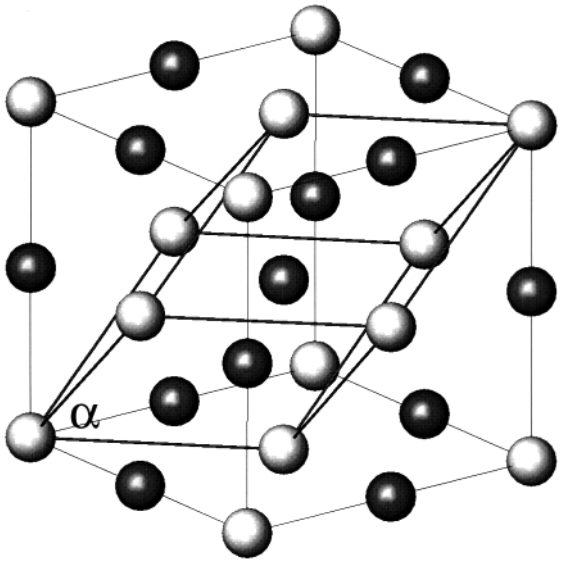

Figure 3. The relationship between the unit cells of the rocksalt structure (thin lines) and the rhombohedrally distorted CsCl one (thick lines). A continuous transition from the rocksalt to the cubic CsCl arrangement can be achieved by gradually increasing the interaxial angle α to 90°.

Table 3. The variation of the volume ratio of the CsCl and rocksalt structures (V_{CsCl}/V_{RS}) with the ratio of the radii of the two ionic species (r_M/r_X).

Radius ratio	Ion–ion contact direction		Volume ratio
r_M/r_X	Rocksalt	CsCl	V_{CsCl}/V_{RS}
$r_M/r_X < \sqrt{2}-1 = 0.414$	[110]	[100]	$V_{CsCl}/V_{RS} = \sqrt{2} = 1.414$
$0.732 \geqslant r_M/r_X \geqslant 0.414$	[100]	[100]	$V_{CsCl}/V_{RS} = \dfrac{4}{(1+r_M/r_X)^3}$
$r_M/r_X > \sqrt{3}-1 = 0.732$	[100]	[111]	$V_{CsCl}/V_{RS} = \sqrt{3}/9 = 0.770$

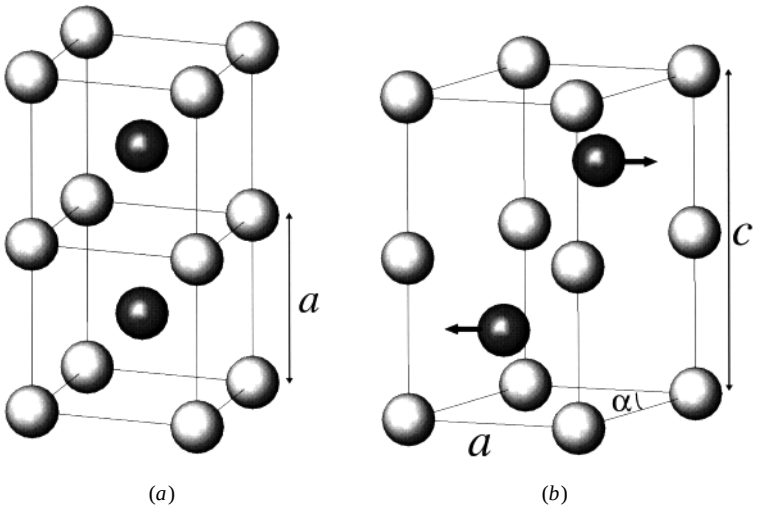

Figure 4. The relationship between (*a*) the CsCl structure of AgF-II and (*b*) the anti-NiAs structure of AgF-III. The darker and lighter spheres represent the Ag^+ and F^-, respectively. The transition from the CsCl structure to the anti-NiAs structure can be considered as a decrease in the illustrated interaxial angle α from 90° to 60° (corresponding to an increase in the conventional hexagonal angle γ from 90° to 120°) and displacements of the cations in the directions shown by the arrows in (*b*).

between nearest-neighbour unlike ions in the [111] and [001] directions, respectively. For AgF, the value $r_{Ag^+}/r_{F^-} = 0.865$ is, therefore, consistent with the greater packing density of the eightfold coordinated CsCl arrangement. However, the measured volume ratio at ambient pressure obtained by extrapolating the compressibility data to zero pressure in figure 1 is estimated to be $V_{CsCl}/V_{RS} = 0.884(4)$. This value which is lower than expected is also observed in those alkali halide compounds which undergo a rocksalt → CsCl transition under pressure (see [29] and references therein).

As illustrated in figure 4, the structural transformation from CsCl → anti-NiAs on decreasing pressure can be visualized as an increase in the 'hexagonal' inter-axial angle γ from 90° to 120° and a shift in the positions of the Ag^+ in alternate CsCl unit cells from $\frac{1}{2}, \frac{1}{2}, \frac{1}{4}$ and $\frac{1}{2}, \frac{1}{2}, \frac{3}{4}$ in the hexagonal setting to $\frac{1}{3}, \frac{2}{3}, \frac{1}{4}$ and $\frac{2}{3}, \frac{1}{3}, \frac{3}{4}$, i.e. by $\frac{1}{6}, -\frac{1}{6}, 0$ in alternate directions perpendicular to the z-axis. The subsequent transition from anti-NiAs to rocksalt is then accomplished by shifting $\frac{3}{4}$ of the layers perpendicular to the z-axis by $\pm(\frac{1}{3}, \frac{2}{3}, 0)$ in the hexagonal setting, as discussed earlier in this section. To understand the

presence of the anti-NiAs-structured phase AgF-III and an intermediary between the CsCl and rocksalt phases on decreasing pressure, we note that the rocksalt structure comprises of two ccp sublattices separated by $\frac{1}{2}, \frac{1}{2}, \frac{1}{2}$. However, if the two ionic species are of comparable size (as in AgF), the overall structure is close to simple cubic and the packing density is relatively low. As a result, distortions of the rocksalt structure, such as the $\langle 111 \rangle$ route to the CsCl arrangement, are expected under pressure. As discussed above, the ideal NiAs structure with $c/a = \sqrt{8}/3$ has an identical packing density to rocksalt and, similarly, can be distorted to form more (or less) efficient packing schemes. If $c/a < \sqrt{8}/3$ then the anion and cation centred polyhedra are both compressed along the z-axis but the structure becomes less densely packed than rocksalt. This is typified by the high-pressure phase with the NiAs arrangement reported in the III–V compound AlAs [30], which has $c/a = 1.597$ (i.e. lower than ideal) and can be considered as an intermediate between the ambient tetrahedrally coordinated zincblende structure and the octahedrally coordinated rocksalt one, which might be expected to occur at even higher pressures. Conversely, an arrangement with $c/a > \sqrt{8}/3$ shows a tendency towards close packing and, on these geometrical grounds alone, the observation of $c/a \sim 1.92$ in anti-NiAs-structured AgF is consistent with its appearance between the sixfold and eightfold coordinated arrangements. Indeed, closer examination of the structural behaviour of AgF-III within its (limited) stability range (figure 5) illustrates that the c-axis behaves anomalously by decreasing on decreasing pressure, such that c/a tends towards the 'ideal' value as the unit cell volume increases.

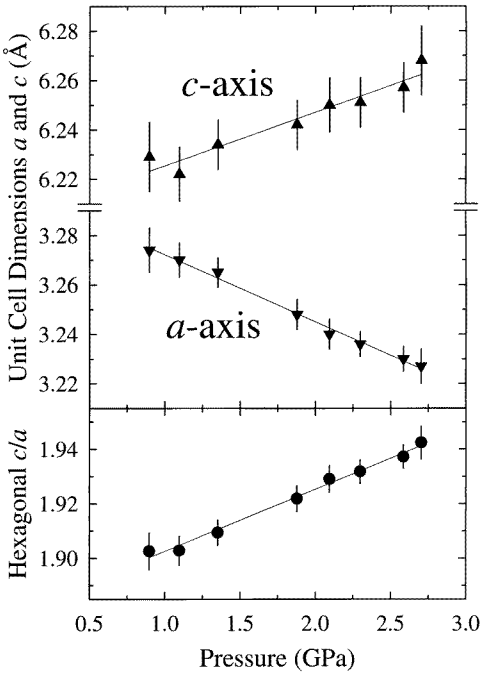

Figure 5. The pressure variation of the a- and c-axis dimensions of the anti-NiAs-structured phase AgF-III, which result in a decrease in c/a with decreasing pressure.

Finally, it is of interest to compare the high-pressure behaviour of AgF with that observed in the other I–VII compounds. Unfortunately, the presence of a high-pressure phase with the CsCl structure has only been observed in AgCl at $p = \sim 17$ GPa and $T \sim 470$ K

[6]. In this compound, two intermediate phases are observed between the rocksalt and CsCl-structured phases which possess the monoclinic KOH-type structure (space group $P2/c$) and orthorhombic TlI arrangement (space group $Cmcm$) [6, 31]. AgBr and AgI also transforms from the rocksalt structure to a KOH-type structure at elevated pressure [31]. The adoption of these particular structures has been attributed to the influence of the partial covalent character of AgCl, AgBr and AgI, such that the tendency towards directional bonds is accommodated by forming structures which are normally characterized by non-spherical ions (OH^- in KOH and e^- lone pair of Tl^+ in TlI) [6]. The markedly different high-pressure structural behaviour of AgF may then be explained by its significantly higher ionicity ($f = 0.894$ on the Phillips scale [32]) compared to AgCl ($f = 0.856$), AgBr ($f = 0.850$) and AgI ($f = 0.770$). On these grounds, AgF is more closely related to the rocksalt structured alkali halide compounds, especially those in which the anions and cations are of roughly comparable size. However, NaF, NaCl and all four halides of both K^+ and Rb^+ undergo direct rocksalt $\rightarrow$ CsCl transitions under increasing pressure [33]. It would be interesting to perform further studies on *decreasing* pressure to determine whether the anti-NiAs structure is also stabilized in these compounds.

5. Conclusions

Intuitively, the presence of an anti-NiAs-structured phase as elevated pressures in AgF is surprising, since it is not an arrangement normally associated with predominantly ionic compounds. However, whilst topologically equivalent to NiAs, the ionic configuration in the anti-NiAs structured phase AgF-III is sufficiently different that comparisons with other isostructural compounds are somewhat misleading. In particular, the electrostatic repulsion between the F^- arranged along z-axis leads to an elongated hexagonal unit cell with c/a considerably larger than both the 'ideal' value of $\sqrt{8}/3$ and the values in the range 1.2–1.7 observed in metal–metalloid compounds with the NiAs structure [22, 34]. As a consequence, the (anti-) NiAs arrangement is more densely packed than rocksalt. This fact, coupled with the reasonably direct modes of transformation, explain its presence as an intermediate phase between the rocksalt and CsCl-structured ones. Recent theoretical calculations of the relative lattice energies of AgCl, AgBr and AgI using several candidate binary structures [8] concluded that the NiAs arrangement is preferred to its antitype with the 'best' values of $c/a \sim 1.4$–1.5. However, it was found to have considerably higher energy than the rocksalt arrangement and not to be a serious contender as a high-pressure phase in these three compounds. It would be interesting to test this theoretical approach by establishing whether the anti-NiAs structure observed in this experimental study is indeed found to be energetically favourable in AgF.

Acknowledgment

One of us (PB) wishes to thank the Swedish Foundation for International Cooperation in Research and Higher Education for financial support.

References

[1] Wyckoff R W G 1963 *Crystal Structures* vol 1 (New York: Interscience)
[2] Keen D A and Hull S 1993 *J. Phys.: Condens. Matter* **5** 23
[3] Hull S and Keen D A 1993 *Europhys. Lett.* **23** 129
[4] Hull S and Keen D A 1994 *Phys. Rev.* B **50** 5868

[5] Keen D A, Hull S, Hayes W and Gardner N J G 1996 *Phys. Rev. Lett.* **77** 4914
[6] Kusaba K, Syono Y, Kikegawa T and Shimomura O 1995 *J. Chem. Solids* **56** 751
[7] Hsueh H C, MacLean J R, Guo G Y, Lee M H, Clark S J, Ackland G J and Crain J 1995 *Phys. Rev.* B **51** 12 216
[8] Nunes G S, Allen P B and Martins J L 1998 *Phys. Rev.* B **57** 5098
[9] Chelikowsky J R and Burdett J K 1986 *Phys. Rev. Lett.* **56** 961
[10] Chelikowsky J R 1987 *Phys. Rev.* B **35** 1174
[11] Christensen N E, Satpathy S and Pawlowska Z 1987 *Phys. Rev.* B **36** 1032
[12] Crain J, Piltz R O, Ackland G J, Clark S J, Payne M C, Milman V, Lin J S, Hatton P D and Nam Y H 1994 *Phys. Rev.* B **50** 8389
[13] Vaidya S N and Kennedy G C 1971 *J. Chem. Solids* **32** 951
[14] Halleck P M, Jamieson J C and Pistorius C W F T 1972 *J. Phys. C: Solid State Phys.* **33** 769
[15] Jamieson J C, Halleck P M, Roof R B and Pistorius C W F T 1975 *J. Phys. Chem. Solids* **36** 939
[16] Sears V F 1992 *Neutron News* **3** 26
[17] Besson J M, Nelmes R J, Hamel G, Loveday J S, Weill G and Hull S 1992 *Physica* B **180/181** 907
[18] Decker D L 1979 *J. Appl. Phys.* **42** 3239
[19] Hull S, Smith R I, David W I F, Hannon A C, Mayers J and Cywinski R 1992 *Physica* C **180/181** 1000
[20] David W I F, Ibberson R M and Matthewman J C 1992 *Rutherford Appleton Laboratory Report* RAL-92-031
[21] Brown P J and Matthewman J C 1992 *Rutherford Appleton Laboratory Report* RAL-92-032
[22] Mak T C W and Zhou G D 1992 *Crystallography in Modern Chemistry* (New York: Wiley)
[23] Thompson J G, Rae A D, Withers R L, Welberry T R and Willis A C 1988 *J. Phys. C: Solid State Phys.* **21** 4007
[24] Froyen S and Cohen M L 1983 *Phys. Rev.* B **28** 3258
[25] Hyde B G and Andersson S 1989 *Inorganic Crystal Structures* (New York: Wiley)
[26] Onodera A, Nakai Y, Kawano S and Achiwa N 1992 *High Temp.- High Press* **24** 55
[27] Watanabe M, Tokonami M and Morimoto N 1977 *Acta Crystallogr.* A **33** 294
[28] Shannon R D and Prewitt C T 1969 *Acta Crystallogr.* B **25** 925
[29] Yagi T, Suzuki T and Akimoto S-I 1983 *J. Chem. Solids* **44** 135
[30] Greene R G, Luo H, Ti L and Ruoff A L 1994 *Phys. Rev. Lett.* **72** 2045
[31] Hull S and Keen D A in preparation
[32] Phillips J C 1970 *Rev. Mod. Phys.* **42** 317
[33] Merrill L 1977 *J. Phys. Chem. Ref. Data* **6** 1205
[34] Matthias B T, Geballe T H and Compton V B 1963 *Rev. Mod. Phys.* **35** 1
[35] Birch F 1978 *J. Geophys. Res.* **83** 1257